

Biaxial Murine Vaginal Remodeling with Reproductive Aging

Shelby E. White

Tulane University, Department of Biomedical Engineering 6823 St Charles Ave
New Orleans, LA 70118
swhite18@tulane.edu

Jasmine X. Kiley

Tulane University, Department of Biology 6823 St Charles Ave
New Orleans, LA 70118
jkiley@tulane.edu

Bruna Visniauskas, Ph.D.

Tulane University, Department of Pharmacology 1430 Tulane Ave
New Orleans, LA 70118
bvisniauskas@tulane.edu

Sarah H. Lindsey, Ph.D.

Tulane University, Department of Pharmacology 1430 Tulane Ave
New Orleans, LA 70118
lindsey@tulane.edu

Kristin S. Miller, Ph.D.*

Tulane University, Department of Biomedical Engineering 6823 St Charles Ave
New Orleans, LA 70118
kmille11@tulane.edu

Abstract

Higher reproductive age is associated with increased risk of gestational diabetes, preeclampsia, and severe vaginal tearing during delivery. Further, menopause is associated with vaginal stiffening. However, the mechanical properties of the vagina during reproductive aging before the onset of menopause are unknown. Therefore, the first objective of this study was to quantify the biaxial mechanical properties of the nulliparous murine vagina with reproductive aging. Menopause is further associated with a decrease in elastic fiber content, which may contribute to the vaginal stiffening. Hence, our second objective was to determine the effect of elastic fiber disruption on the biaxial vaginal mechanical properties. To accomplish this, vaginal samples from CD-1 mice aged 2-14 months underwent extension-inflation testing protocols (n=64 total; n=16/age group). Then, half of the samples were randomly allocated to undergo elastic fiber fragmentation via elastase digestion (n=32 total; 8/age group) to evaluate the role of elastic fibers. The material stiffness increased with reproductive age in both the circumferential and axial directions within the control and elastase-treated vaginas. The vagina demonstrated anisotropic mechanical behavior, and anisotropy increased with age. In summary, vaginal remodeling with reproductive age included increased direction-dependent material stiffness, which further increased following elastic fiber disruption. Further work is needed to quantify vaginal remodeling during pregnancy and postpartum with reproductive aging to better understand how age-related vaginal remodeling may contribute to increased risk of vaginal tearing.

1. INTRODUCTION

Nine times more women are delaying child bearing to after 35 years old compared to 4 decades ago [1]. Increased reproductive age is associated with increased risk of gestational diabetes, high blood pressure, preeclampsia, delivering pre-term, and greater risk of obstetric injury such as severe vaginal tearing (2nd degree tearing during childbirth) [2-5]. Further, increased age is associated with various pathologies such as sexual dysfunction and vaginal atrophy [6, 7]. While the etiology of the increased risk for obstetric trauma or pathology development is not well-defined, remodeling of the extracellular matrix (ECM) with age may contribute [8]. The vagina is a fibromuscular hollow organ that is composed of smooth muscle cells, fibroblasts, collagen, elastic fibers, and nonfibrous extracellular components such as glycosaminoglycans. With the onset of menopause in the human reproductive tissues, collagen content increases while elastic fibers undergo fragmentation [7, 9]. Furthermore, the ewe vagina is materially stiffer with menopause when compared to pregnant samples [10]. While this material stiffening is likely due to microstructural and compositional changes, such as decreased skeletal muscle and fragmentation of elastic fibers, baseline microstructural comparisons in the nonpregnant premenopausal groups are unknown. Prior works compared mechanical changes between pre- and postmenopausal samples, however, progressive remodeling of mechanical function during the reproductive years remains unknown [10-12]. While mice do not sustain birth injuries, studies in rodents may provide further insights into the possible structural and biomechanical processes during reproductive aging due to well documented relationships of human and mouse aging, predictive estrous cycles, and various genetic modifications [13-16]. At 8-10 months of age, mice undergo prolonged labor that closely mimics that observed in human women [17]. Hence, murine models are valuable tools to better understand cellular and molecular processes that contribute to reproductive aging and increased reproductive complications [16, 18, 19]. While preliminary analysis of the uterus and cervix was reported [17], vaginal remodeling during reproductive aging has not been evaluated to the authors' knowledge.

The vagina must be able to withstand various intra-abdominal pressures due to childbearing, walking, lifting, and defecating, all of which induce loads in multiple directions [20]. However, to date, vaginal mechanical function is predominately evaluated in a single direction [21-23]. While uniaxial protocols provide valuable information, uniaxial testing cannot account for the multiaxial physiologic loads. Towards this end, the rat vagina demonstrated higher stress values and lower stretches in the circumferential direction compared to the axial in both active and passive conditions [24]. Direction-dependent changes in vaginal mechanical properties with reproductive aging, however, are unknown. To better inform clinical practices and potentially understand disease progression, the direction-dependent nature of soft tissues must be carefully considered. Furthermore, elastic fibers permit soft tissues to stretch and recoil following mechanical loading [25, 26]. Therefore, elastic fibers may contribute to vaginal remodeling during pregnancy and progressive aging [8, 27, 28]. Previously, disruption of elastic fibers with elastase increased the outer diameter, decreased the compliance, and increased circumferential stress of the 4-6 months C57BL/6 murine vagina [29]. Furthermore, the C57BL/6 murine vagina has a higher area fraction of elastic fibers in the axial direction compared to the circumferential [30]. However, it is not known if elastic fiber composition, and thus the biaxial mechanical contribution of elastic fibers, changes with reproductive aging.

Therefore, the first objective of this study was to quantify the biaxial mechanical properties of the murine vagina with reproductive aging. We hypothesized that vaginal material stiffness increases with reproductive age. Further, we hypothesized that the circumferential direction would be stiffer than the axial direction across all ages. Our second objective was to determine the effect of elastic fiber disruption on the biaxial mechanical properties of the murine vagina. This was accomplished by treating the vagina with elastase, which is an enzyme that degrades elastin [29, 31]. We hypothesized that elastic fiber disruption would increase vaginal material stiffness within each age group. Additionally, we hypothesized that elastase will have a larger effect in the circumferential direction [29]. Furthermore, aging is a dynamic process that is associated with various independent characteristics, such as body mass [32, 33]. Regression models are a

useful tool to determine potential correlations of complex biological processes. Therefore, multiple regression analyses were employed to evaluate potential correlations, independent predictor variables, and potential confounding effects that may occur with reproductive aging. Ultimately, this study offers a first step in better understanding vaginal remodeling with reproductive age and following elastic fiber disruption. Further, this study comprises an initial approach towards understanding correlations and predictor variables during vaginal remodeling in multiple directions.

2. METHODS

2.1 Pressure catheterization

N=9 female nulliparous CD-1 mice (2-14 months) were used to measure intravaginal pressure with a balloon catheter (Fig 1C). Pressure measurements were taken at 2 months of age and repeated at 3-week increments until 14 months of age. All pressure measurements were taken at estrus. Mice were anesthetized with 4% isoflurane in 100% oxygen to measure intravaginal pressure [30]. A 3 mm balloon was fabricated with polyvinyl chloride and secured with 6-0 silk sutures around a 1.25 mm aluminum tube. A 3-way stop cock connected the balloon catheter to a disposable pressure transducer (InnoLogic #GP 91051) and 3 mL syringe filled with autoclaved deionized water. The pressure transducer was integrated to a laptop that recorded the pressure readings (PowerLab and LabChart8, ADInstruments, Colorado Springs, CO, USA). To facilitate the pressure measurements, 1.5 mL of water was then pushed into the balloon via the syringe to obtain the baseline pressure measurement. A pressure of the inflated balloon in ambient air was recorded. The balloon was inserted into the vaginal canal and the resultant pressure was noted. The vaginal pressure was measured as the change in in pressure between ambient conditions and the pressure of the balloon once in contact with the vaginal wall. For each experiment, the pressure measurements were performed 3 times on each animal and averaged for one data point [30].

2.2 Animal Care

An n of 64 (2-3 months n=16; 4-6 months n=16; 7-9 months n=16; 10-14 months n=16) nulliparous female CD-1 mice at estrus were housed in a 12-hour light/dark cycle and fed a normal chow diet with Tulane University Institutional Animal Care and Use Committee (IACUC) approval (Fig 1). Mice aged 2-14 months represented the human age equivalents to 18-62 years of age as reported previously [15]. Estrous cycle phase was determined visually by lifting the tail and determining the width of the vaginal opening, as described by Byers et al., 2012 [34]. Prior to the mechanical testing, each mouse was weighed on a digital scale and then euthanized.

2.3 Dissection

70% ethanol was applied to the abdomen and wicked the fur down. Dissection scissors were used to cut the underlying skin and muscle layer vertically from pubis to sternum. Lateral cuts under the ribs and above the pubis created an “I-cut” and exposed the abdomen. Using blunt forceps, intestines were carefully moved towards the sternum to better visualize the reproductive system. Visceral fat around the uterine horns was cut away using micro-scissors. The pubic symphysis was then cut with curved dissection scissors and the fascial tethering was removed from the anterior vagina and urethra. To remove the urethra from the vaginal wall, the bladder was held in tension with blunt forceps and micro-scissors gently removed the urethra. The uterine horns were then cut 3 mm away from the uterine body and held in tension to better visualize the connections between the vaginal wall and rectum. Curved dissection scissors were used to cut around the external vaginal opening. The vagina was then removed from the body and placed in a dish filled with 4°C Hank’s Balanced Saline Solution (HBSS). A singular cut was made between the cervix and vagina to excise the vagina from the cervix and uterine horns.

2.4 Sample Preparation and Cannulation

Following dissection, each end of the excised vagina was cannulated onto a 3.75 mm (outer diameter) cannula situated within a custom biaxial extension-inflation pressure myograph (Danish MyoTechnologies, Aarhus, Denmark) [30, 35-38]. Two silk 6-0 sutures were tied to both ends of the cannulated vagina and

secured with blunt forceps. The cervical end of the vagina was cannulated onto the fluid flow inlet and the external opening side onto the outlet to mimic the natural flow of menstruation or childbirth. Samples were maintained in a bath of HBSS kept at 4°C during cannulation [39, 40].

2.5 Biomechanical Testing

Biaxial extension-inflation testing assessed the biaxial mechanical properties while maintaining the native cell-matrix interactions and preserving the tubular geometry (Fig 1). To induce passive conditions, the testing media was replaced with a Krebs solution without calcium. Smooth muscle tone was removed by adding 2 mM of a calcium-chelating agent, egtazic acid (EGTA), to the organ bath. The organ was then incubated for 30 minutes [35]. The unloaded pressure was identified as the pressure at which the largest change in outer diameter occurred. The vagina was then set to the estimated physiologic length and unloaded pressure. At a rate of 10 $\mu\text{m/s}$, the axial length was decreased until there was a minimal change in axial force. This observed length was defined as the unloaded length and the axial force was zeroed [30, 36]. The physiologic length was identified where the transducer-measured forces held constant over a range of increasing physiologic pressures and recorded during the experiment. Initial pressure-diameter preconditioning minimized hysteresis with cyclic pressurization from 0 mmHg to the mean measured *in vivo* pressure over 5 cycles at 1.5 mmHg/s [41, 42]. Further, axial preconditioning was performed via force-length testing wherein the vagina was axially extended from -2% to +2% of the physiologic length at a constant pressure ($\frac{1}{3}$ of the maximum pressure (6 mmHg)) [26,32]. Five cycles of pressurization (0-15 mmHg) at the physiologic length, followed by axial extension (10 $\mu\text{m/s}$) from 2% below to 2% above the physiologic length at a constant pressure preconditioned the vagina [36]. The tissue equilibrated for 10 minutes at the physiologic length, followed by re-establishment of the unloaded configuration [35]. The vagina was subjected to cyclic pressure-diameter over a range of physiologic pressures (0-18 mmHg) at the physiologic length and about -2% and +2% of the length [36]. Force length testing confirmed the vagina was tested at the physiologic length. A linear micrometer extended the vagina axially from -2% of the

physiologic length to +2% at four constant pressures: a tare pressure (3 mmHg), $\frac{1}{3}$ of the maximum pressure (6 mmHg), $\frac{2}{3}$ of the maximum pressure (12 mmHg), and the maximum pressure (18 mmHg) [30, 41, 42].

2.6 Tissue Allocation and Treatment

Prior to mechanical testing, a random number generator randomly allocated vaginal samples to either elastase treatment or control conditions. In the event of elastase treatment, the vagina was treated intraluminally with 15 U enzymatic elastase digestion for 45 minutes [29]. Protocols for pressure diameter testing and force length were repeated. Pressure diameter and force length testing were then conducted using EGTA treatment as described above [29].

2.7 Ultrasound

Vaginal wall thickness was measured using ultrasound images taken at the unloaded configuration for the control and elastase conditions using the Vevo2100 ultrasound system (FUJIFILM VisualSonics Inc., Toronto, ON, Canada) with a 40MHz center frequency transducer (LZ550) [43]. Short-axis B-mode ultrasound images were obtained at the proximal region of the vagina, as this is the portion optically tracked during pressure diameter testing. ImageJ (NIH, Bethesda, MD) determined the thickness of the vaginal wall by tracing the inner and outer wall with 25 transmural lines [43].

2.8 Data Analysis

For the data analysis and adaptation of the equations presented herein, the vagina is assumed to be cylindrical in shape [29]. The unloaded volume (V) was determined using the unloaded outer radius (R_o), unloaded thickness (H), and the unloaded length (L) under both the control and elastase conditions (equation 1).

$$V = \pi(R_o^2 - (R_o - H)^2)L \quad (\text{Equation 1})$$

Assuming the vagina is an incompressible soft tissue, the deformed inner radius (r_i) was determined by equation 2 with the regional length (l) and measured deformed outer radius (r_o).

$$r_i = \sqrt{r_o^2 - \frac{V}{\pi l}} \quad (\text{Equation 2})$$

The wall-averaged circumferential (σ_θ) and axial (σ_z) Cauchy stresses (equation 3 and 4, respectively) were determined using previously described variables as well as the intraluminal pressure (P) and transducer measured force (F_t) [44, 45].

$$\sigma_\theta = \frac{Pr_i}{r_o - r_i} \quad (\text{Equation 3})$$

$$\sigma_z = \frac{F_t + \pi Pr_i^2}{\pi(r_o^2 - r_i^2)} \quad (\text{Equation 4})$$

The circumferential stretch ratio was determined as the deformed vaginal wall radius in relation to the unloaded configuration (equation 5). The axial stretch was defined as the axial length as compared to the unloaded axial length (equation 6).

$$\lambda_\theta = \frac{(r_i + r_o)/2}{(R_i - R_o)/2} \quad (\text{Equation 5})$$

$$\lambda_z = \frac{l}{L} \quad (\text{Equation 6})$$

Circumferential and axial material stiffness were calculated around the estimated physiologic length and pressure as determined by balloon catheterization. In the circumferential and axial direction, the material stiffness was calculated by using the MATLAB polyfit linear function to describe the region from the lower physiologic pressure (LPB) and upper physiologic pressure boundary (UPB), which corresponds to +/- 1 standard deviation of the physiologic pressure (Fig 1D) [45, 46].

2.8 Statistics

Statistics were performed by hypothesis using R software (version 3.6.2). To ensure normality, Shapiro-Wilks tests were completed for each data set. A 1-way ANOVA (age) evaluated potential differences in the vaginal pressure across the increasing age groups. An additional 1-way ANOVA (age) identified

differences in the body mass of the mice with reproductive aging. When appropriate, Tukey's post hoc Honest Significant Differences (HSD) tests followed the 1-way ANOVA. Further, a 1-way ANOVA (age) evaluated differences in the physiologic length of the vagina under testing conditions. For the first hypothesis, a 2-way ANOVA (age, direction) evaluated potential direction-dependent differences in material stiffness as a function of reproductive age. Additionally, anisotropy was further investigated by determining the ratio of the circumferential material stiffness and the axial material stiffness. The ratio of the direction-dependent material stiffness was analyzed utilizing a 1-way ANOVA (age). To evaluate the role of elastic fibers, a 2-way ANOVA (elastase, direction) was used. When appropriate, Tukey's post hoc HSD tests were performed. When significant interactions between variables were identified, simple plots were constructed to determine main effects, as determined by non-zero slopes, and the presence of complex interactions, or variable lines that intersect [32, 47]. Furthermore, we sought to determine potential correlations and confounding effects that often accompany age such as increased in body mass [32, 48]. To understand such potential relationships, and to adjust for postulated direction dependence, regression analysis was performed for the vaginal material stiffness in the circumferential and axial directions. Pearson correlations within each direction further evaluated potential relationships between body mass, reproductive age, and vaginal material stiffness. Multiple linear regression models were performed to determine independent predictors of material stiffness. Regression models were assessed by p-values and predictive capability by standardized Beta (B) coefficients. Statistical significance level was set at $p < 0.05$, and a statistical trend at $p < 0.10$. Results are presented as mean +/- standard error of the mean (SEM).

3. RESULTS

3.1 Intravaginal Pressure, Physiologic Length, and Body Mass

For the datasets described herein, the Shapiro-Wilks test suggested that the error of the data was normally distributed ($p > 0.05$). Based on prior literature [20, 48], it was postulated that with reproductive aging, biological variables such as vaginal pressure and weight (body mass) would increase. A 1-way ANOVA (age) identified a statistical trend with increasing vaginal pressure with reproductive age ($p = 0.06$ (Fig 2A)).

Further, a 1-way ANOVA (age) identified that body mass was a significant factor with reproductive aging ($p < 0.001$). Tukey's post hoc HSD test identified a significantly greater body mass in the 4-6 months ($p = 0.01$), 7-9 months ($p < 0.001$), and 10-14 months ($p < 0.001$) mice as compared to the 2-3 months. Additionally, the physiologic length of the vagina did not statistically differ with age in either the control or elastase treatment group ($p = 0.47$; $p = 0.39$, respectively). Though to note, the average physiologic length in the control conditions were as follows for the 2-3 months, 4-6 months, 7-9 months, and 10-14 months: 5.91 ± 0.72 mm, 5.82 ± 0.98 mm, 6.63 ± 0.69 mm, and 5.54 ± 0.67 mm. Additionally, the physiologic length for the elastase conditions were recorded as the following (average \pm standard deviation): 6.19 ± 0.82 mm, 6.28 ± 0.89 mm, 6.15 ± 1.4 mm, and 5.39 ± 0.94 mm. Further, the weight in the 7-9 months ($p = 0.02$) and 10-14 months was significantly greater than the 4-6 months mice. Additionally, the 10-14 months mice had a significantly larger mass than that of the 7-9 months mice ($p = 0.03$) (Fig 2B).

3.2 Objective 1: Direction-Dependent Changes with Reproductive Age

A 2-way ANOVA (age, direction) identified significant differences in the material stiffness with respect to reproductive age ($p < 0.001$) and direction ($p < 0.001$). The interaction between age and direction was also statistically significant ($p = 0.004$). Post-hoc tests were not performed due to the significant interaction between age and direction. With increased reproductive age, the material stiffness increased in both the circumferential and axial directions (Fig 3A). To investigate the nature of the significant interaction, a simple interaction plot was generated to interpret the relationship between age and directional material stiffness. The increased distance between the circumferential and axial values of material stiffness with progressive aging (Fig 3B), suggest that anisotropy increased with reproductive aging. Additionally, the ratio of the direction-dependent material stiffness values (a measure of anisotropy) as a function of increasing reproductive age was identified as a statistical trend ($p = 0.09$).

3.3 Objective 2: Direction-Dependent Changes Following Elastic Fiber Disruption

To investigate how elastic fiber disruption contributed to direction-dependent material stiffness, a 2-way ANOVA (elastase, direction) was used within each age group. For the 2-3 months, elastase ($p < 0.001$), direction ($p < 0.001$), as well as the interaction ($p = 0.001$) were significant (Fig 4A). For the 4-6 months, elastase ($p < 0.001$) and direction ($p < 0.001$) were significant, however, the interaction term was not statistically significant, but demonstrated a statistical trend ($p = 0.08$) (Fig 4B). The 7-9 months had main effects for elastase ($p = 0.011$) and direction ($p < 0.001$), with no significant interaction ($p = 0.128$) (Fig 4D). In the 10-14 months age group, elastase ($p = 0.04$) and direction ($p < 0.001$) were significant with no significant interaction ($p = 0.40$) (Fig 4E).

Due to significant interactions in the 2-3 months and 4-6 months, a simple interaction plot was constructed that observed main effects in both the circumferential and axial direction, as indicated by the non-zero slope from control to elastase material stiffness (Fig 4C). No complex interactions were observed within the simple plot (Fig 4C). Elastase treatment increased the material stiffness in the circumferential and axial direction (Fig 4C). Further, the circumferential material stiffness was greater than that of the axial material stiffness (Fig 4C). For the 7-9 months and 10-14 months groups, which did not have significant interactions, Tukey's post hoc HSD tests were conducted. Post-hoc tests in the 7-9 months group observed that under control conditions, the circumferential material stiffness was significantly greater than the axial direction ($p = 0.005$). Additionally, under elastase conditions, the circumferential material stiffness was significantly greater than that of the axial material stiffness ($p < 0.001$). Additional t-tests in the 7-9 months group did not demonstrate significant differences in the circumferential control vs circumferential elastase ($p = 0.155$) or in the axial control vs axial elastase ($p = 0.77$) (Fig 4D). Similarly for the 10-14 months, under control conditions, the circumferential material stiffness was significantly greater than the axial direction ($p < 0.001$). With elastase treatment, the circumferential material stiffness was significantly greater than the axial material stiffness ($p < 0.001$). Additionally, the circumferential elastase vs the circumferential control was identified as a significant trend ($p = 0.064$). Further post hoc analysis did not demonstrate significant differences in the axial control vs axial elastase ($p = 0.672$) (Fig 4D).

3.4 Multiple Regression

Regression analyses were completed to account for potential confounding factors that are associated with reproductive aging, such as increasing body mass while adjusting for the hypothesized direction-dependent material stiffness. First, Pearson (r) correlations investigated potential univariate associations between reproductive age, body mass, and material stiffness in each direction (Table 1). For the control circumferential material stiffness, reproductive age ($r=0.86$; $p=0.008$) and body mass ($r=0.73$; $p=0.02$) were strongly correlated. For the axial control material stiffness, strong positive correlations were identified between the reproductive age ($r=0.83$; $p<0.001$) and body mass ($r=0.77$; $p=0.01$). Additionally, the circumferential elastase material stiffness was strongly associated with reproductive age ($r=0.74$; $p<0.001$) and body mass ($r=0.57$; $p=0.005$). Further correlations between the elastase treated samples in the axial material stiffness with reproductive age ($r=0.76$; $p=0.02$) and body mass ($r=0.79$; $p=0.004$) were identified.

Next, multiple linear regression analysis was employed to determine independent predictors of material stiffness in both directions [32]. Models evaluated reproductive age, elastase treatment, and body mass as potential independent predictors for material stiffness in each direction (Table 2). The residuals of the models did not depart from normality ($p>0.05$). Within the circumferential direction (Table 2), the model fit the data moderately well ($R^2=0.74$). Reproductive age ($p<0.001$), elastase treatment ($p<0.001$), and body mass ($p=0.02$) were significant independent predictors of circumferential material stiffness. With the model, variables with the highest beta values (B) indicate the strongest predictive term. Of the variables chosen, reproductive age was the strongest predictor of circumferential material stiffness ($B=0.54$; $p<0.001$). Body mass also positively predicted the circumferential material stiffness, though to a lesser degree than age ($B=0.27$; $p=0.02$). Further, the regression model identified elastase as a negative predictor ($B=-0.48$; $p<0.001$). For the regression analyses, elastase treatment was randomly given a -1 value and control treatment was given a +1 value. This inverse relationship indicates where elastase treatment resulted in an increased material stiffness. The model fit the axial direction data moderately well ($R^2=0.68$) (Table

2). Each independent predictor was statistically significant: reproductive age ($p=0.02$), elastase treatment ($p<0.001$), and body mass ($p=0.03$). Elastase treatment was the strongest predictor, as determined by the B values ($B=-0.48$; $p<0.001$). Body mass was an additional strong positive predictor of axial material stiffness ($B=0.42$; $p=0.003$) as well as reproductive age ($B=0.3$; $p=0.02$).

To determine the presence of interactions among the independent predictor variables (age, elastase, body mass), each model previously constructed was adjusted for either elastase treatment or reproductive age. This was completed in both the circumferential and axial direction (Table 3). Model 1 included both reproductive age and elastase as well as the interaction effect of age*elastase. In the circumferential direction, both reproductive age ($p<0.001$) and elastase treatment ($p<0.001$) were determined to be significant. The interaction term was not significant in Model 1. For the axial direction, Model 1 fit the data moderately well ($R^2 = 0.62$). Further, reproductive age ($p<0.001$) and elastase ($p<0.001$) were significant independent predictors. The interaction for Model 1 was not significant in the axial direction. Model 2 included reproductive age, body mass, as well as the interaction term of age*body mass. For the circumferential direction, reproductive age ($p=0.007$) and body mass ($p=0.07$) were significant, and the interaction term was not ($p=0.12$). Model 2 fit the axial direction well, though to a lesser degree ($R^2=0.55$). In the axial direction, age ($p=0.006$), body mass ($p=0.004$), and the interaction term ($p=0.04$) were significant predictors of the axial material stiffness.

4. DISCUSSION

This investigation determined how direction-dependent vaginal mechanical properties change during reproductive aging. Data supported our hypothesis that material stiffness increased with reproductive age in both the circumferential and axial directions (Fig 3). The observed material stiffening with reproductive age may be due to changes in the microstructural composition or organization of the vagina. Burnett et al. categorized human cadaveric pelvic floor samples from younger (less than 52) or older (greater than 52) women and observed that pelvic floor muscles underwent age-related stiffening due to an accumulation of

collagen and advanced glycation end products in the extracellular matrix [49]. A study by Amargant et al. observed that mice aged 14-17 months had stiffer ovaries compared mice aged 1-3 months and that the ovarian stiffness was dependent on collagen content [50]. While the processes are not fully understood, this age-related fibrosis was conserved when investigating the human ovary [51, 52]. To date, changes in extracellular matrix content and organization, such as collagen fiber content, accumulation of collagen crosslinks, and collagen subtype ratios, with vaginal reproductive aging remains unknown. Further work would be greatly impacted by investigating the processes that cause the material stiffening as this would aid in understanding potential etiologies of increased obstetric injury with increasing reproductive age.

Furthermore, the observed material stiffness with reproductive aging may, in part, be influenced by changes in repetitive mechanical loading, such as intra-abdominal pressures or weight gain. Body mass significantly increased with reproductive age and was significantly correlated with material stiffness in both the circumferential and axial directions (Table 1). Body mass may be correlated with material stiffness due to the increased load on the vagina over time as women with a higher body mass index exhibit materially stiffer vaginas [48]. Similar to lifting heavy objects, the increased load due to body mass may induce elastic fiber fragmentation or damage to other extracellular matrix components, potentially contributing to increased material stiffness. Furthermore, body mass demonstrated a greater predictive capability in the axial direction, which may suggest that the load from the increased mass was distributed more along the axial direction than the circumferential or that more remodeling occurred in this direction. However, further analysis is needed to support or refute these hypotheses to better understand potential links between reproductive aging, loading, stiffness, and matrix composition. For example, future work utilizing animal models would benefit from controlled weight experiments to decouple potential roles in body mass and reproductive age in vaginal remodeling. While increased age is a primary risk factor for increased intra-abdominal pressure in human women and may also contribute to vaginal remodeling, the *in vivo* vaginal pressure in this study did not significantly differ with age [5, 53]. Previously, age was associated with increased intra-abdominal pressure but the study design did not control for factors such as menopausal

status, obesity, or gravidity, all of which may also influence the intra-abdominal pressure [53]. While it is possible for increased repetitive mechanical loads due to body mass and intra-abdominal pressure to influence material stiffness of the tissues, further studies are needed to clearly define the role of each factor while adjusting for other potentially confounding variables.

While quantification of microstructure was outside of the scope of the current study, vaginal mechanical response following disruption of elastic fibers was investigated. Interestingly, post-hoc analyses in the 7-9 months and 10-14 months did not demonstrate significant differences between the control and elastase treatment groups (Fig 4). However, the simple plot showed elastase had a significant effect in the 2-3 months and 4-6 months age groups. Taken together, these findings suggested that younger mice may either have a higher content of elastic fibers or higher fraction of intact, mechanically functional elastic fibers than the older counterparts (Fig 4C-E). In the human vagina, menopause is associated with fragmented elastic fibers [54, 55]. Thus, as mice age towards the human equivalent of menopause (10-14 months), elastic fibers may be fragmented or damaged from repetitive loading [7, 56, 57]. Since the vagina is an estrogen-dependent organ, it is highly probable that changes in steroid hormones may augment production and removal of collagen and elastic fibers [49, 58-60]. C57BL/6 mice at 11-12 months had reduced progesterone levels, decreased ovarian and uterine function, and decreased viable oocytes and implantation sites during early pregnancy compared to 3-7 month old mice [61]. Further work is needed to better understand potential biochemical changes with reproductive aging in non-pregnant and pregnant mice to identify prospective correlations with extracellular matrix composition and mechanical function. However, Tsukahara et al. demonstrated that skin from ovariectomized mice display elastic fiber fragmentation and decreased elasticity compared to mice with normal estrogen levels [62]. This further supports the need to better understand interactions between steroid hormones and elastic fiber content.

The vagina exhibited increasingly anisotropic behavior throughout reproductive aging, as indicated by the increased distance between the circumferential and axial material stiffness curves (Fig 3). Similarly, the 2-

3 months nulliparous rat vagina demonstrated greater stress values calculated in the circumferential direction compared to the axial direction. The authors suggested that the anisotropic behavior was likely due to collagen and smooth muscle fiber organization, as well direction specific innervations of the vaginal wall [24]. Additionally, elastic fibers may constrain collagen undulation in addition to providing tissue resilience and recoil. Thus, anisotropic organization of elastic fibers may also contribute to direction-dependent mechanical properties in the vaginal wall. Towards this end, direction-dependent changes were observed following elastic fiber disruption, as indicated by the slope difference in the circumferential and axial directions (Fig 3C). Circumferential material stiffness was larger than the axial for both the 7-9 months and 10-14 months age groups (Fig 3C). Clark et al. reported that the elastic fiber area fraction in C57BL/6 mice was greater in the axial direction than the circumferential direction and that collagen fibers were more highly aligned towards the circumferential axis [30]. Thus, the disruption of elastic fibers may result in a decrease in collagen fiber undulation, thereby increasing the circumferential material stiffness [38, 40, 63]. Additionally, Akintunde et al. observed elastase treatment in 4-6 months C57BL/6 mice increased structural stiffness in only the circumferential direction as well as decreased vaginal compliance [29]. Further, these direction dependent changes in material stiffness motivated quantifying anisotropy as the ratio of circumferential to axial material stiffness, which was identified as a statistical trend herein. This trend may have implications for the direction-dependent vaginal microstructure and remodeling rates of the microstructural components in each direction. Taken together, these data demonstrate the need for comprehensive investigations on the microstructure and composition across the entire vagina to draw further direction dependent conclusions. While the study herein provided a preliminary understanding of the direction-dependent properties, future studies may further apply this knowledge to better understand progression of diseases such as sexual dysfunction or vaginal atrophy and better inform biomaterial therapeutics [7, 54].

The study is not without limitations. The elastase concentration and incubation time were selected following a pilot study that delineated the optimal treatment conditions, which decreased the mechanical

properties while consistently providing repeatable testing conditions. The pilot study work was previously utilized by Akintunde et al., where histological analysis demonstrated significantly less elastin area fractions, though some elastin remained in the tissue. Given the purpose of this study was to investigate the effects of elastic fiber fragmentation, the same concentration and exposure time provided a reasonable first step in understanding the role of elastic fibers in vaginal mechanics. Further, a large body of work suggests that the mechanical properties and microstructural composition of the vagina change with pregnancy and hormones [49, 58, 64]. Additionally, it is acknowledged that reproductive aging is associated with difficulty in becoming pregnant, increased rates of complications during pregnancy, and maladaptive postpartum healing [2-5, 55]. The biomechanical origin of these age-related complications is of high interest to the field and served as motivation of this study. However, to fully understand the etiology of these complications, baseline characterization of the nonpregnant samples with aging was needed. Additionally, the work herein measured the passive mechanical properties of the murine vagina, or the properties that do not include contractility from smooth muscle cells. While this offers a first step in understanding vaginal mechanics with increasing reproductive age, it does not fully capture the *in vivo* properties of the vagina. Future work is needed consider the smooth muscle contractility of the vaginal wall and how these properties change with increasing reproductive age.

Furthermore, while the mouse does offer several advantages as an animal model, there are limitations regarding the translation to human studies. One of which is mice do not naturally sustain injuries during birth. While the biomechanics of pregnancy and postpartum healing were not considered in the scope of this work, future studies should carefully consider size variations of the birth canal and how that influences the mechanical properties of the vagina. Additionally, the mouse is a quadruped animal as opposed to humans, which are bipedal. This distinction does present possible variations in the function of some connective tissues in the reproductive system; namely the levator ani in bipedal animals functions to provide vaginal support whereas in quadrupeds the levator ani functions in the movement of the tail [60]. While the levator ani offers a clear distinction between the two groups, there are a large number of

similarities between the structure and function of the vaginal connective tissues between the rodent and human, which makes the rodent an acceptable model for reproductive studies. Finally, an assumption of incompressibility of the vaginal tissue was made to calculate thickness and subsequently used in the volume and radius equations to calculate the directional stress and stretch. This assumption was previously employed in prior biomechanical work in the murine vagina [29, 30, 36, 65, 66]. Using ultrasound analysis, Clark et al. observed the volume of the C57BL6 x 129SvEv murine vagina did not change with physiologically-relevant loads (0-15 mmHg), suggesting that the assumption is reasonable for the CD-1 murine vagina [65]. Future work to validate this assumption may be possible in the future as mechanical testing systems become more integrated with real-time imaging systems. As the testing system currently stands, reasonably assuming incompressibility offers a preliminary outlook to how the vaginal mechanics change with increased reproductive age and fragmented elastic fibers.

5. CONCLUSIONS:

In summary, vaginal material stiffness increased with reproductive age and disruption of elastic fibers. Disruption of elastic fibers with reproductive aging may contribute to increased material stiffness, offering a potential structural hypothesis for the increased rate of vaginal injuries in older mothers. Further work is needed to better understand direction-dependent changes in vaginal composition and microstructure with reproductive aging in nonpregnant and pregnant mice.

FUNDING

The NSF Award no. 1947770 (K.S.M) funded this work.

ACKNOWLEDGMENTS

We acknowledge Dr. Akinjide Akintunde for guidance on the guidance on linear regression analysis.

- [1] Matthews, T. P., Zhang, C., Yao, D.-K., Maslov, K., and Wang, L. V., 2014, "Label-free photoacoustic microscopy of peripheral nerves," *Journal of biomedical optics*, 19(1), p. 16004.
- [2] Rahmanou, P., Caudwell-Hall, J., Kamisan Atan, I., and Dietz, H. P., 2016, "The association between maternal age at first delivery and risk of obstetric trauma," *American Journal of Obstetrics and Gynecology*, 215(4), pp. 451.e451-451.e457.
- [3] Lao, T. T., Ho, L.-F., Chan, B. C. P., and Leung, W.-C., 2006, "Maternal age and prevalence of gestational diabetes mellitus," *Diabetes care*, 29(4), pp. 948-949.
- [4] Gaillard, R., Bakker, R., Steegers, E. A. P., Hofman, A., and Jaddoe, V. W. V., 2011, "Maternal Age During Pregnancy Is Associated With Third Trimester Blood Pressure Level: The Generation R Study," *American journal of hypertension*, 24(9), pp. 1046-1053.
- [5] Yadav, H., and Lee, N., 2013, "Maternal factors in predicting low birth weight babies," *Medical journal of Malaysia*, 68(1), pp. 44-47.
- [6] Lethaby, A., Ayeleke, R. O., and Roberts, H., 2016, "Local oestrogen for vaginal atrophy in postmenopausal women," *The Cochrane database of systematic reviews*, 2016(8), p. CD001500.
- [7] Castelo-Branco, C., Cancelo, M. J., Villero, J., Nohales, F., and Juliá, M. D., 2005, "Management of post-menopausal vaginal atrophy and atrophic vaginitis," *Maturitas*, 52(1), pp. 46-52.
- [8] Ferruzzi, J., Collins, M., Yeh, A., and Humphrey, J., 2011, "Mechanical assessment of elastin integrity in fibrillin-1-deficient carotid arteries: implication for Marfan syndrome," *Cardiovascular Research*, 92(2), pp. 287-295.
- [9] Moalli, P. A., Talarico, L. C., Sung, V. W., Klingensmith, W. L., Shand, S. H., Meyn, L. A., and Watkins, S. C., 2004, "Impact of menopause on collagen subtypes in the arcus tendineous fasciae pelvis," *American journal of obstetrics and gynecology*, 190(3), pp. 620-627.
- [10] Kochová, P., Hympanová, L., Rynkevic, R., Cimrman, R., Tonar, Z., Deprest, J., and Kalis, V., 2019, "The histological microstructure and in vitro mechanical properties of pregnant and postmenopausal ewe perineal body," *Menopause (New York, N.Y.)*, 26(11), pp. 1289-1301.
- [11] Alperin, M., Burnett, L., Lukacz, E., and Brubaker, L., 2019, "The mysteries of menopause and urogynecologic health: clinical and scientific gaps," *Menopause*, 26(1), pp. 103-111.
- [12] Ripperda, C., Maldonado, P., Acevedo, J., Keller, P., Akgul, Y., Shelton, J., and Word, R. A., 2017, "Vaginal estrogen: a dual-edged sword in postoperative healing of the vaginal wall," *North American Menopause Society*, 24(7), pp. 838-849.
- [13] Cui, S., Chesson, C., and Hope, R., 1993, "Genetic variation within and between strains of outbred Swiss mice," *Lab Animals*, 27, pp. 116-123.
- [14] Nelson, J., Felicio, P., Randall, K., Sims, C., and Finch, E., 1982, "A Longitudinal Study of Estrous Cyclicity in Aging C57/6J Mice: Cycle, Frequency, Length, and Vaginal Cytology," *Biology Reproduction*.
- [15] Dutta, S., and Sengupta, P., 2016, "Men and mice: Relating their ages," *Life Sciences*, 152(1), pp. 244-248.
- [16] Fox, J. G., 2007, *The Mouse in biomedical research*, Academic Press, Amsterdam ;
- [17] Patel, R., Moffatt, J. D., Mourmoura, E., Demaison, L., Seed, P. T., Poston, L., and Tribe, R. M., 2017, "Effect of reproductive ageing on pregnant mouse uterus and cervix: Effect of reproductive ageing on pregnant uterus and cervix," *The Journal of physiology*, 595(6), pp. 2065-2084.

- [18] Rice, M., and O'Brien, S., 1980, "Genetic variance of laboratory outbred Swiss mice," *Nature*, 283, pp. 157-161.
- [19] Chia, R., Achilli, F., Festing, M., and Fisher, E., 2005, "The origins and uses of mouse outbred stocks," *Nature Genetics*, 37, pp. 1181-1186.
- [20] O'Dell, K. K., Morse, A. N., Crawford, S. L., and Howard, A., 2007, "Vaginal pressure during lifting, floor exercises, jogging, and use of hydraulic exercise machines," *International Urogynecology Journal*, 18(12), pp. 1481-1489.
- [21] Goh, J. T. W., 2002, "Biomechanical Properties of Prolapsed Vaginal Tissue in Pre- and Postmenopausal Women," *Including Pelvic Floor Dysfunction*, 13(2), pp. 76-79.
- [22] Rahn, D. D., Ruff, M. D., Brown, S. A., Tibbals, H. F., and Word, R. A., 2008, "Biomechanical properties of the vaginal wall: effect of pregnancy, elastic fiber deficiency, and pelvic organ prolapse," *American journal of obstetrics and gynecology*, 198(5), pp. 590.e591-590.e596.
- [23] Martins, P., Pena, E., Calvo, B., Doblare, M., Mascarenhas, T., Jorge, N., and Ferreira, A., 2010, "Prediction of Nonlinear Elastic Behavior of Vaginal Tissue: Experimental Results and Model Formation," *Computational Methods of Biomechanics and Biomedical Engineering*, 13(3), pp. 317-337.
- [24] Huntington, A., Rizzuto, E., Abramowitch, S., Prete, Z., and De Vita, R., 2018, "Anisotropy of the Passive and Active Rat Vagina Under Biaxial Loading," *Annals of Biomedical Engineering*, 47, pp. 272-281.
- [25] Leppert, P. C., 1991, "Three-dimensional structures of uterine elastic fibers: scanning electron microscopic studies," *Connective tissue research*, 27(1), p. 15.
- [26] Sherratt, M., 2009, "Tissue elasticity and the ageing elastic fibre," *The Official Journal of the American Aging Association*, 31(4), pp. 305-325.
- [27] Liu, M., Zhang, P., Chen, M., Zhang, W., Yu, L., Yang, X.-C., and Fan, Q., 2012, "Aging might increase myocardial ischemia / reperfusion-induced apoptosis in humans and rats," *The Official Journal of the American Aging Association*, 34(3), pp. 621-632.
- [28] Kerkhof, M. H., Hendriks, M. L., and Brölmann, H. A. M., 2009, "Changes in connective tissue in patients with pelvic organ prolapse-a review of the current literature," *International Urogynecology Journal*.
- [29] Akintunde, A., Robison, K., Capone, D., Desrosiers, L., Knoepp, L., and Miller, K., 2018, "Effects of Elastase Digestion on the Murine Vaginal Wall Biaxial Mechanical Response," *American Society of Mechanical Engineers*, 141(2).
- [30] Clark, G. L., Pokutta-Paskaleva, A. P., Lawrence, D. J., Lindsey, S. H., Desrosiers, L., Knoepp, L. R., Bayer, C. L., Gleason, R. L., and Miller, K. S., 2019, "Smooth muscle regional contribution to vaginal wall function," *Interface focus*, 9(4), p. 20190025.
- [31] Dobrin, P. B., and Mrkvicka, R., 1994, "Failure of Elastin or Collagen as Possible Critical Connective Tissue Alterations Underlying Aneurysmal Dilatation," *Vascular*, 2(4), pp. 484-488.
- [32] Corden, B., Keenan, N. G., de Marvao, A. S. M., Dawes, T. J. W., DeCesare, A., Diamond, T., Durighel, G., Hughes, A. D., Cook, S. A., and O'Regan, D. P., 2013, "Body Fat Is Associated With Reduced Aortic Stiffness Until Middle Age," *Hypertension*, 61(6), pp. 1322-1327.
- [33] Lopez, S. O., Eberhart, R. C., Zimmern, P. E., and Chuong, C.-J., 2015, "Influence of body mass index on the biomechanical properties of the human prolapsed anterior vaginal wall," *International urogynecology journal*, 26(4), pp. 519-525.

- [34] Byers, S., 2012, "Mouse Estrous Cycle Identification Tool and Images," PLoS ONE, 7(4).
- [35] Conway, C. K., Qureshi, H. J., Morris, V. L., Danso, E. K., Desrosiers, L., Knoepp, L. R., Goergen, C. J., and Miller, K. S., 2019, "Biaxial biomechanical properties of the nonpregnant murine cervix and uterus," *Journal of Biomechanics*, 94.
- [36] Robison, K., Conway, C., Desrosiers, L., Knoepp, L., and Miller, K., 2017, "Biaxial Mechanical Assessment of the Murine Vaginal Wall Using Extension-Inflation Testing," *Journal of Biomechanical Engineering*, 139(10).
- [37] Caulk, A., Nepiyushchikh, Z., Shaw, R., Dixon, B., and Gleason, R., 2015, "Quantification of the passive and active biaxial mechanical behavior and microstructural organization of rat thoracic ducts," *Royal Society Interface*, 12.
- [38] Ferruzzi, J., Collins, M., Yeh, A., and Humphrey, J., 2011, "Mechanical assessment of elastin integrity in fibrillin-1-deficient carotid arteries: implications for Marfan Syndrome," *Cardiovascular Research*, 92(2), pp. 287-295.
- [39] Lei, L., Song, Y., and Chen, R., 2007, "Biomechanical properties of prolapsed vaginal tissue in pre- and postmenopausal women," *International Urogynecology Journal*, 18(6), pp. 603-607.
- [40] Murtada, S., Ferruzzi, J., Yanagisawa, H., and Humphrey, J., 2016, "Reduced Biaxial Contractility in the Descending Thoracic Aorta of Fibulin-5 Deficient Mice," *Journal of Biomechanical Engineering*, 138(5).
- [41] Amin, M., Le, V., and Wagenseil, J., 2012, "Mechanical Testing of Mouse Carotid Arteries: from Newborn to Adult," *Journal of Visual Experiments*(60).
- [42] Ferruzzi, J., Bersi, M. R., and Humphrey, J. D., 2013, "Biomechanical Phenotyping of Central Arteries in Health and Disease: Advantages of and Methods for Murine Models," *Annals of biomedical engineering*, 41(7), pp. 1311-1330.
- [43] Panayi, D. C., Digesu, G. A., Tekkis, P., Fernando, R., and Khullar, V., 2010, "Ultrasound measurement of vaginal wall thickness: a novel and reliable technique," *International Urogynecology Journal*, 21(10), pp. 1265-1270.
- [44] Ferruzzi, J., Bersi, M., and Humphrey, J., 2013, "Biomechanical phenotyping of Central Arteries in Health and Disease: Advantages of and Methods for Murine Models," *Annals of Biomedical Engineering*, 41(7), pp. 1311-1330.
- [45] Humphrey, J., 2002, *Cardiovascular Solid Mechanics: Cells, Tissues, and Organs*, Springer, New York.
- [46] Wagenseil, J. E., and Mecham, R. P., 2012, "Elastin in Large Artery Stiffness and Hypertension," *Journal of cardiovascular translational research*, 5(3), pp. 264-273.
- [47] Preacher, K. J., and Kelley, K., 2011, "Effect Size Measures for Mediation Models: Quantitative Strategies for Communicating Indirect Effects," *Psychol Methods*, 16(2), pp. 93-115.
- [48] Lopez, S., Eberhart, R., Zimmern, P., and Chuong, C.-J., 2015, "Influence of body mass index on the biomechanical properties of the human prolapsed anterior vaginal wall," *Including Pelvic Floor Dysfunction*, 26(4), pp. 519-525.
- [49] Burnett, L. A., Cook, M., Shah, S., Michelle Wong, M., Kado, D. M., and Alperin, M., 2020, "Age-associated changes in the mechanical properties of human cadaveric pelvic floor muscles," *Journal of biomechanics*, 98.

- [50] Amargant, F., Manuel, S. L., Tu, Q., Parkes, W. S., Rivas, F., Zhou, L. T., Rowley, J. E., Villanueva, C. E., Hornick, J. E., Shekhawat, G. S., Wei, J. J., Pavone, M. E., Hall, A. R., Pritchard, M. T., and Duncan, F. E., 2020, "Ovarian stiffness increases with age in the mammalian ovary and depends on collagen and hyaluronan matrices," *Aging cell*, 19(11), pp. e13259-n/a.
- [51] Briley, S. M., Jasti, S., McCracken, J. M., Hornick, J. E., Fegley, B., Pritchard, M. T., and Duncan, F. E., 2016, "Reproductive age-associated fibrosis in the stroma of the mammalian ovary," *Reproduction (Cambridge, England)*, 152(3), pp. 245-260.
- [52] McCloskey, C. W., Cook, D. P., Kelly, B. S., Azzi, F., Allen, C. H., Forsyth, A., Upham, J., Rayner, K. J., Gray, D. A., Boyd, R. W., Murugkar, S., Lo, B., Trudel, D., Senterman, M. K., and Vanderhyden, B. C., 2020, "Metformin Abrogates Age-Associated Ovarian Fibrosis," *Clinical cancer research*, 26(3), pp. 632-642.
- [53] Kılıç, B., Yapıcı, N., Yapıcı, F., Kavaklı, A. S., Kudsioğlu, T., Kılıç, A., and Aykaç, Z., 2020, "Factors associated with increased intra-abdominal pressure in patients undergoing cardiac surgery," *Türk göğüs kalp damar cerrahisi dergisi*, 28(1), pp. 134-142.
- [54] Pandit, G. L., and Ouslander, G. J., 1997, "Postmenopausal Vaginal Atrophy and Atrophic Vaginitis," *The American Journal of the Medical Sciences*, 314(4), pp. 228-231.
- [55] Sarrel, P. M., 1990, "Sexuality and Menopause," *Obstetrics & Gynecology*, 75(Supplement), p. 31S.
- [56] Karam, J. A., Vazquez, D. V., Lin, V. K., and Zimmern, P. E., 2007, "Elastin expression and elastic fibre width in the anterior vaginal wall of postmenopausal women with and without prolapse," *BJU international*, 100(2), pp. 346-350.
- [57] Florian-Rodriguez, M., Chin, K., Hamner, J., Acevedo, J., Keller, P., and Word, R. A., 2019, "Effect of Protease Inhibitors in Healing of the Vaginal Wall," *Scientific reports*, 9(1), pp. 12354-12310.
- [58] Catanzarite, T., Bremner, S., Barlow, C. L., Bou-Malham, L., O'Connor, S., and Alperin, M., 2018, "Pelvic muscles' mechanical response to strains in the absence and presence of pregnancy-induced adaptations in a rat model," *American journal of obstetrics and gynecology*, 218(5), pp. 512.e511-512.e519.
- [59] Alperin, M. M. D. M. S., Lawley, D. M. B. S., Esparza, M. C. B. S., and Lieber, R. L. P., 2015, "Pregnancy-induced adaptations in the intrinsic structure of rat pelvic floor muscles," *American journal of obstetrics and gynecology*, 213(2), pp. 191.e191-191.e197.
- [60] Burnett, L. A., Boscolo, F. S., Laurent, L. C., Wong, M., and Alperin, M., 2019, "Uncovering changes in proteomic signature of rat pelvic floor muscles in pregnancy."
- [61] Li, M.-Q., Yao, M.-N., Yan, J.-Q., Li, Z.-L., Gu, X.-W., Lin, S., Hu, W., and Yang, Z.-M., 2017, "The decline of pregnancy rate and abnormal uterine responsiveness of steroid hormones in aging mice," *Reproductive biology*, 17(4), pp. 305-311.
- [62] Tsukahara, K., Nakagawa, H., Moriwaki, S., Kakuo, S., Ohuchi, A., Takema, Y., and Imokawa, G., 2004, "Ovariectomy is sufficient to accelerate spontaneous skin ageing and to stimulate ultraviolet irradiation-induced photoageing of murine skin," *British journal of dermatology (1951)*, 151(5), pp. 984-994.
- [63] Ferruzzi, J., Bersi, M. R., Mecham, R. P., Ramirez, F., Yanagisawa, H., Tellides, G., and Humphrey, J. D., 2016, "Loss of elastic fiber integrity compromises common carotid artery function: Implications for vascular aging," *Artery Research*, 14, pp. 41-52.

[64] Alperin, M. M. D. M. S., Kaddis, T. B. S., Pichika, R. P., Esparza, M. C. B. S., and Lieber, R. L. P., 2016, "Pregnancy-induced adaptations in intramuscular extracellular matrix of rat pelvic floor muscles," *American journal of obstetrics and gynecology*, 215(2), pp. 210.e211-210.e217.

[65] Clark-Patterson, G., McGuire, J., Desrosiers, L., Knoepp, L., De Vita, R., and Miller, K., 2021, "Investigation of Murine Vaginal Creep Response to Altered Mechanical Loads," *Journal of Biomechanical Engineering*.

[66] Clark-Patterson, G., Roy, S., Desrosiers, L., Knoepp, L., Sen, A., and Miller, K., 2021, "Role of Fibulin-5 insufficiency and prolapse progression on murine vaginal Biomechanical function " *Scientific Reports*.

Table Caption List

Table 1: Univariate associations within the circumferential and axial directions. Age and body mass were significantly correlated with the circumferential and axial material stiffness. Each set of variables maintained significance under the elastase treatment conditions.

Table 2: Independent predictors of material stiffness for the circumferential and axial direction. The model fitted each direction reasonably well, with a modestly higher R^2 value in the circumferential direction ($R^2=0.74$ vs $R^2=0.68$). Age, elastase treatment, and body mass were significant factors for both directions. The predictive capability of each variable was assessed by the standardized beta (B) values. Age was the variable with the highest predictive capacity for the circumferential direction, however, elastase treatment demonstrated the highest predictive capability for the axial direction.

Table 3: Independent predictors of material stiffness for the circumferential and axial direction with interactions. To adjust for body mass and elastase treatment, two models were constructed for regression analysis. Model 1 consisted of age, elastase treatment, and the interaction factor. Model 1 fitted each direction moderately well, with a modestly higher R^2 value ($R^2=0.72$ vs $R^2=0.62$). Within Model 1, the variable with the highest predictive capability was elastase ($B=-0.48$). Within the axial direction, elastase treatment also had the highest predictive capability ($B=-0.16$). The interaction factor was not significant in either direction. Model 2 consisted of age, body mass, and their interaction factor. Model 2 fitted each direction moderately well with a higher R^2 value in the circumferential direction ($R^2=0.62$ vs $R^2=0.55$). Body mass was no longer a significant predictor variable

for the circumferential direction. Meanwhile age maintained to be the highest predictor variable for both directions ($B=0.83$ for both directions). The interaction factor was significant in the axial direction, potentially suggesting that effect of body mass changes with age or that the effect of body mass becomes more significant with age.

Figure Caption List

Figure 1: A total of 64 female CD-1 mice at estrus aged 2-3 (n=16), 4-6 (n=16), 7-9 (n=16), and 10-14 (n=16) months were used (A; human year age correlations) [16]. Two experimental extension-inflation protocols were employed: the control passive characterization and 15 U elastase digestion that fragments the elastic fibers followed by passivation (B). Prior to mechanical testing a total of 9 mice/ age group underwent pressure catheterization to determine the *in vivo* vaginal pressure (C). This pressure measurement was then used to determine the circumferential and axial material stiffness (in vivo pressure +/- 1 standard deviation) (D).

Figure 2: A total of 64 female CD-1 mice at estrus aged 2-3 (n=16), 4-6 (n=16), 7-9 (n=16), and 10-14 (n=16) months were used (A; human year age correlations) [16]. Two experimental extension-inflation protocols were employed: the control passive characterization and 15 U elastase digestion that fragments the elastic fibers followed by passivation (B). Prior to mechanical testing a total of 9 mice/ age group underwent pressure catheterization to determine the *in vivo* vaginal pressure (C). This pressure measurement was then used to determine the circumferential and axial material stiffness (in vivo pressure +/- 1 standard deviation) (D). Statistical significance of $p<0.05$ was represented by *, $p<0.01$ **, and $p<0.001$ ***.

Figure 3: A 2-way ANOVA (age, direction) identified significant differences in the material stiffness with age ($p<0.001$), direction ($p<0.001$), and the interaction between age and direction ($p=0.004$). The material stiffness increased with reproductive age in the circumferential (black) and axial direction (navy) (A). The circumferential material stiffness was greater than that of the axial direction within each age group. Further, anisotropy increased with reproductive age as indicated by the increased difference in the circumferential (black) and axial (blue) relations to material stiffness (B).

Figure 4: Circumferential and axial material stiffness from the intact control (circumferential – black; axial – navy) and post-elastase treated (circumferential – grey; axial – light blue) vaginas are shown at 2-3 months (circles; A), 4-6 months (triangles; B), 7-9 months (square; D), and 10-14 months (diamonds; E). While post hoc tests were not appropriate in the 2-3 ($p=0.001$) and 4-6 months ($p=0.09$) due to significant and trending interactions, relationships between elastase treatment and direction were investigated via simple plot visualization (C). For the 2-3 months and 4-6 months age groups, elastase and direction are main effects in determining the material stiffness of the murine vagina, as evidenced by the non-zero slopes. No complex interactions observed. The circumferential direction (black) is materially stiffer than the axial (blue), in both the control and elastase condition (C). Post hoc t-tests were performed in the 7-9 months group and demonstrated significant differences in the circumferential control vs axial control ($p=0.009$) as well as the circumferential elastase and axial elastase ($p<0.001$). Additional post hoc analyses were performed for the 10-14 months and similarly observed differences in the circumferential control vs axial control ($p<0.001$) as well as the circumferential elastase and axial elastase ($p<0.001$). Further, the 10-14 months circumferential elastase was greater than the circumferential control material stiffness and was identified as a significant trend ($p=0.064$). Statistical significance of $p<0.05$ was represented by *, $p<0.01$ **, and $p<0.001$ ***.

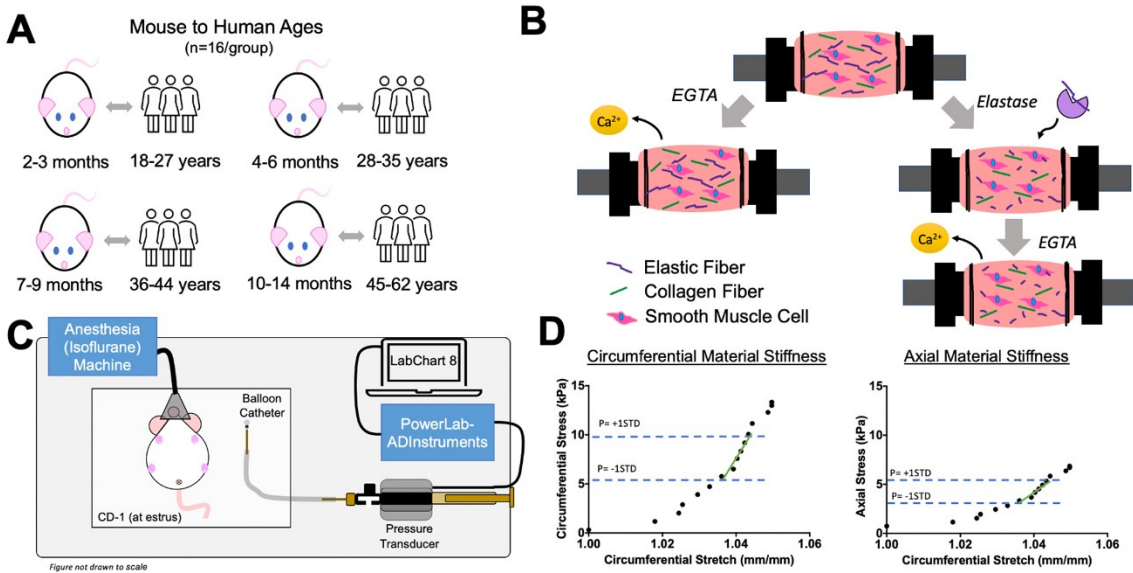


Figure 1: A total of 64 female CD-1 mice at estrus aged 2-3 (n=16), 4-6 (n=16), 7-9 (n=16), and 10-14 (n=16) months were used (A; human year age correlations) [16]. Two experimental extension-inflation protocols were employed: the control passive characterization and 15 U elastase digestion that fragments the elastic fibers followed by passivation (B). Prior to mechanical testing a total of 9 mice/ age group underwent pressure catheterization to determine the *in vivo* vaginal pressure (C). This pressure measurement was then used to determine the circumferential and axial material stiffness (in vivo pressure \pm 1 standard deviation) (D).

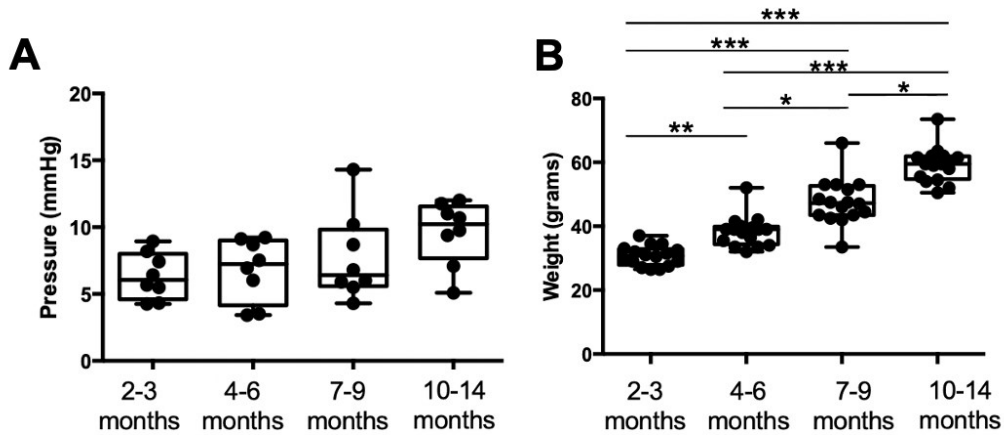


Figure 2: A 1-way ANOVA (age) evaluated the statistical differences in intravaginal pressure quantified in anesthetized mice. No significant differences were noted with reproductive age ($p=0.06$) (A). Body mass, measured prior to mechanical testing, significantly increased with reproductive age ($p<0.001$). Post hoc Tukey's HSD test identified significant differences in the 2-3 months as compared to the 4-6 months ($p=0.01$), 7-9 months ($p<0.001$), and 10-14 months ($p<0.001$). Additionally, the 7-9 months ($p=0.02$) and 10-14 months ($p<0.001$) had significantly greater weight than the 4-6 months. Finally, the 10-14 months weight was significantly greater than the 7-9 months ($p=0.03$) (B). Statistical significance of $p<0.05$ was represented by *, $p<0.01$ **, and $p<0.001$ ***.

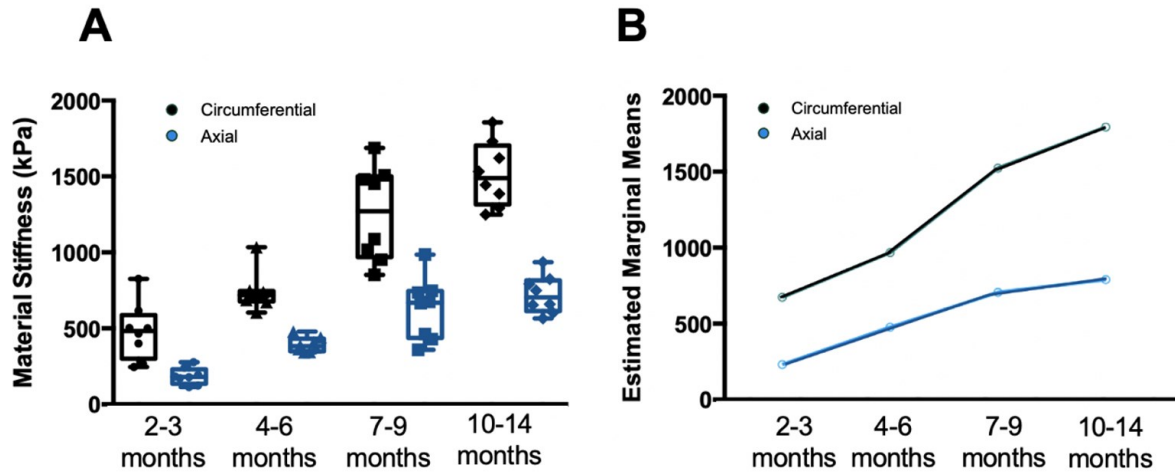


Figure 3: A 2-way ANOVA (age, direction) identified significant differences in the material stiffness with age ($p < 0.001$), direction ($p < 0.001$), and the interaction between age and direction ($p = 0.004$). The material stiffness increased with reproductive age in the circumferential (black) and axial direction (navy) (A). The circumferential material stiffness was greater than that of the axial direction within each age group. Further, anisotropy increased with reproductive age as indicated by the increased difference in the circumferential (black) and axial (blue) relations to material stiffness (B).

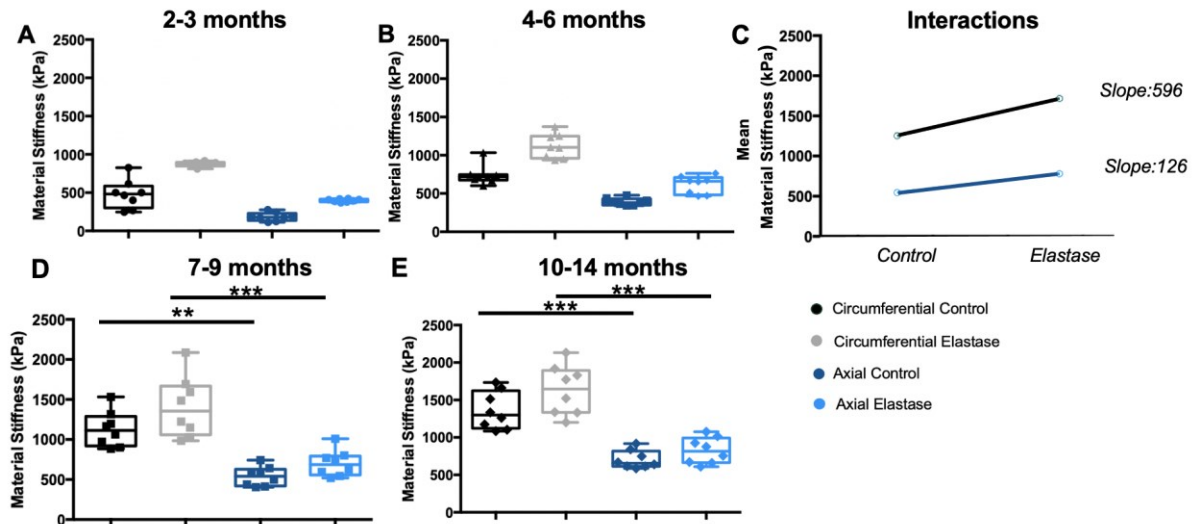


Figure 4: Circumferential and axial material stiffness from the intact control (circumferential – black; axial – navy) and post-elastase treated (circumferential – grey; axial – light blue) vaginas are shown at 2-3 months (circles; A), 4-6 months (triangles; B), 7-9 months (square; D), and 10-14 months (diamonds; E). While post hoc tests were not appropriate in the 2-3 ($p=0.001$) and 4-6 months ($p=0.07$) due to significant and trending interactions, relationships between elastase treatment and direction were investigated via simple plot visualization (C). For the 2-3 months and 4-6 months age groups, elastase and direction are main effects in determining the material stiffness of the murine vagina, as evidenced by the non-zero slopes. No complex interactions observed. The circumferential direction (black) is materially stiffer than the axial (blue), in both the control and elastase condition (C). Post hoc t-tests were performed in the 7-9 months group and demonstrated significant differences in the circumferential control vs axial control ($p=0.009$) as well as the circumferential elastase and axial elastase ($p<0.001$). Additional post hoc analyses were performed for the 10-14 months and similarly observed differences in the circumferential control vs axial control ($p<0.001$) as well as the circumferential elastase and axial elastase ($p<0.001$). Statistical significance of $p<0.05$ was represented by *, $p<0.01$ **, and $p<0.001$ ***.

Pearson r Correlations with Material Stiffness								
Circumferential				Axial				
	Age		Body Mass		Age		Body Mass	
Control	r=0.86	p=0.008	r=0.73	p=0.02	r=0.83	p<0.001	r=0.77	p=0.01
Elastase	r=0.74	p<0.001	r=0.57	p=0.005	r=0.76	p=0.02	r=0.79	p=0.004

Table 1: Univariate associations within the circumferential and axial directions. Age and body mass were significantly correlated with the circumferential and axial material stiffness. Each set of variables maintained significance under the elastase treatment conditions.

Independent predictors of Material Stiffness				
Circumferential R ² =0.74			Axial R ² =0.68	
	Standardized B Coefficients	p value	Standardized B Coefficients	p value
Age	0.54	p<0.001	0.3	p=0.02
Elastase	-0.38	p<0.001	-0.48	p<0.001
Body Mass	0.27	p=0.02	0.42	p=0.03

Table 2: Independent predictors of material stiffness for the circumferential and axial direction. The model fitted each direction reasonably well, with a modestly higher R² value in the circumferential direction (R²=0.74 vs R²=0.68). Age, elastase treatment, and body mass were significant factors for both directions. The predictive capability of each variable was assessed by the standardized beta (B) values. Age was the variable with the highest predictive capacity for the circumferential direction, however, elastase treatment demonstrated the highest predictive capability for the axial direction.

Independent Predictors of Material Stiffness With interactions					
		Circumferential		Axial	
		Model 1 R ² : 0.72	Model 2 R ² : 0.61	Model 1 R ² : 0.62	Model 2 R ² : 0.55
		Standardized B Coefficients	p-value	Standardized B Coefficients	p-value
Model 1	Age	0.7	p<0.001	0.11	p<0.001
	Elastase	-0.48	p<0.001	-0.16	p<0.001
	Age*Elastase	0.08	P=0.28	0.01	p=0.18
Model 2	Age	0.83	p=0.003	0.83	p=0.006
	Body Mass	0.19	p=0.07	0.75	p=0.004
	Age*Body Mass	0.001	p=0.12	0.001	p=0.04

Table 3: Independent predictors of material stiffness for the circumferential and axial direction with interactions. To adjust for body mass and elastase treatment, two models were constructed for regression analysis. Model 1 consisted of age, elastase treatment, and the interaction factor. Model 1 fitted each direction moderately well, with a modestly higher R² value (R²=0.72 vs R² =0.62). Within Model 1, the variable with the highest predictive capability was elastase (B=-0.48). Within the axial direction, elastase treatment also had the highest predictive capability (B=-0.16). The interaction factor was not significant in either direction. Model 2 consisted of age, body mass, and their interaction factor. Model 2 fitted each direction moderately well with a higher R² value in the circumferential direction (R²=0.62 vs R² =0.55). Body mass was no longer a significant predictor variable for the circumferential direction. Meanwhile age maintained to be the highest predictor variable for both directions (B=0.83 for both directions). The interaction factor was significant in the axial direction, potentially suggesting that effect of body mass changes with age or that the effect of body mass becomes more significant with age.